JOURNAL OF Applied Polymer SCIENCE

Interfacial evaluation of epoxy/carbon nanofiber nanocomposite reinforced with glycidyl methacrylate treated UHMWPE fiber

Mojtaba Ahmadi,[1] Mahmood Masoomi,[1] Somayeh Safi,[2] Omid Zabihi[3]
[1]Department of Chemical Engineering, Isfahan University of Technology, Isfahan, Iran
[2]Department of Textile Engineering, Isfahan University of Technology, Isfahan, Iran
[3]Deakin University, Carbon Nexus, Institute for Frontier Materials, Geelong, Australia
Correspondence to: M. Masoomi (E-mail: mmasoomi@cc.iut.ac.ir)

ABSTRACT: Interface interactions of fiber–matrix play a crucial role in final performance of polymer composites. Herein, in situ polymerization of glycidyl methacrylate (GMA) on the ultrahigh molecular weight polyethylene (UHMWPE) fibers surface was proposed for improving the surface activity and adhesion property of UHMWPE fibers towards carbon nanofibers (CNF)-epoxy nanocomposites. Chemical treatment of UHMWPE fibers was characterized by FTIR, XPS analysis, SEM, and microdroplet tests, confirming that the grafting of poly (GMA) chains on the surface alongside a significant synergy in the interfacial properties. SEM evaluations also exhibited cohesive type of failure for the samples when both GMA-treated UHMWPE fiber and CNF were used to reinforce epoxy matrix. Compared with unmodified composite, a ~319% increase in interfacial shear strength was observed for the samples reinforced with both 5 wt % GMA-grafted UHMWPE and 0.5 wt % of CNF. © 2016 Wiley Periodicals, Inc. J. Appl. Polym. Sci. **2016**, *133*, 43751.

KEYWORDS: composites; fibers; mechanical properties; surfaces and interfaces; thermosets

Received 27 February 2016; accepted 7 April 2016
DOI: 10.1002/app.43751

INTRODUCTION

Recently, UHMWPE fibers have attracted considerable attention for advanced performance polymer composites because of their unique combination of outstanding mechanical, physical, and chemical properties. Moreover, UHMWPE fibers show excellent specific strength and modulus compared to other reinforcing fibers (such as glass and Kevlar fibers) due to their low density (0.97 g/cm^3).[1,2] Such a material could be beneficial in the applications where it is desirable to improve strength and reduce weight simultaneously.[3] Composite materials based on epoxy resin reinforced with UHMWPE fibers are widely used in industrial applications such as military hamlet, body armor, and sport goods.[4] Like other composites, interfacial adhesion is one of the most influential factors affecting the mechanical properties of the composites.[5] However, the smooth and inert characteristics of the UHMWPE fiber surface usually result in a lack of interfacial covalent bonds and low interfacial strength in UHMWPE fiber-reinforced epoxy composites. This property in turn affects the ultimate mechanical properties of composites.[6]

There are two approaches to overcome this type of problem; a common one is to treat the fiber, and another is to operate on the matrix. The first technique is acting on UHMWPE fibers including physical and chemical methods, such as plasma treatment, corona discharge, chemical etching, irradiation-induced grafting, and chemical grafting.[3,7–9] The dispersion of nanoparticles such as carbon nanotubes (CNTs) and carbon nanofibers (CNFs) in the matrix is the second method to improve the adhesion between fiber and matrix. Dispersed nanofiller particles could act as a mechanical interlocking between the fiber and matrix improving fracture toughness as well as the modulus, strength, thermal and electrical properties.[3,8,10,11]

The chemical grafting method has been studied by many researchers in the last few years.[12–16] Sadeghi *et al.*[13] studied the effect of grafting reaction process, involving glycidyl methacrylate (GMA) monomer concentration and time, on the interfacial adhesion of GMA-grafted UHMWPE fiber/epoxy composites. It was shown that the grafting percent was greatly influenced by GMA concentration rather than time variable. Li *et al.*[14] showed that grafting of methacrylic acid and acrylamide on to the UHMWPE fiber surface enhanced interfacial bonding properties. They declared that the active groups grafted on to the fiber surface would supply enough anchor points for the chemical bonding and interaction with various resins or further reactions. According to the results obtained by Yakusheva *et al.*,[17] grafting of acrylic monomers on the UHMWPE fiber surface improved interfacial adhesion, resulting in a better fiber–matrix stress transfer. Wang *et al.*[15] found that chemical grafting of acrylamide on to the UHMWPE fibers surface could improve the

interfacial adhesion between treated fibers and matrix. Zhao *et al.*[16] reported that grafting of UHMWPE fibers with acrylamide monomer using peroxidase increased interfacial shear strength between treated fiber and resin.

Studies related to the enhancement of thermosphysical properties of the epoxy matrix by introduction of the different nanofillers, such as CNF, have been weidly conducted.[5,12,18–24] It was observed a significant improvement in mechanical properties, thermal and electrical conductivity of composite even at very low CNF concentrations. Meanwhile, there have been few reports investigating composite systems that have a CNF/epoxy nanophased polymer matrix with UHMWPE fiber.[25] However, the published work on the simultaneous surface treatment and modification of UHMWPE fiber and epoxy resin is scarce. In our previous work, CNFs dispersed epoxy resin was reinforced with unidirectional GMA-grafted UHMWPE fibers, and tensile and flexural properties improvements in three-component nanocomposites were confirmed by obtained results.[12] Here, we investigate the influence of both a matrix modification by using carbon nanofibers and UHMWPE fiber surface treatment via GMA grafting on the resulting adhesion properties in single fiber model composites. CNFs were selected as nanofillers to modify the epoxy resin properties, due to lower manufacturing costs, large aspect ratio, and high mechanical and electrical properties.[26] To achieve maximum utilization of the properties of nanofibers, uniform dispersion and good wetting of the nanofibers within the matrix have to be ensured. This matter has been widely researched, and several techniques have been proposed to overcome the dispersion problem.[5,27] In our study, the ultrasonic treatment was used in combination with the mechanical stirring to disperse 0.5–1.5 wt % CNFs into the epoxy resin. The microdroplet test and contact angle measurement were used to evaluate the effect of fiber surface treatment and epoxy matrix modification on the interfacial shear strength (IFSS) and the surface properties. The surface morphology of the fibers was investigated by scanning electron microscope (SEM). Besides, the tensile properties of a single UHMWPE fiber before and after chemical treatment were determined using the tensile test.

EXPERIMENTAL

Materials

The UHMWPE fiber utilized in this study was Dyneema SK60 (DSM Co., The Netherlands) with a fiber diameter range of 12–21 μm. Dyneema SK60 has a tensile strength of 2.7 GPa and density of 0.97 g/cm^3. Dibenzoyl peroxide (BPO) as initiator was purchased from Merck Co. (Germany). The epoxy resin used in this work was Araldite LY 5052-1, and the curing agent was Aradur 5052-1 grade that was supplied by Huntsman (Switzerland). Glycidyl methacrylate (GMA, purity of 97%) and Carbon nanofibers (CNF, PR-25-XT-PS) were purchased from Sigma-Aldrich.

Surface Modification of UHMWPE Fibers

Samples of UHMWPE fibers were washed in three steps to remove the commercial sizing prior to use in the GMA grafting process. UHMWPE fibers were treated in a bath containing 1% w/v nonionic detergent (Ultravon GP, Ciba) for 2 h, and then rinsed with distillated water. They were then subjected to Soxhlet extraction with acetone for 2 h and vacuum dried at 60 °C for 12 h. For surface modification, the UHMWPE fibers (∼1 g) were immersed in the treating solution containing GMA (0.25 mol/L) and BPO initiator (0.02 mol/L) for 15 min. Then, the impregnated fibers were transferred to a nitrogen gas–filled reaction vessel, and the grafting reaction was carried out at 100 °C for 2 h. After the reaction, the fibers were evacuated from the vessel and purified by Soxhlet extractor filled with acetone solvent for 24 h to remove the unreacted and homopolymerized GMA from the fiber surface. Finally, the fibers were dried in a vacuum oven at 60 °C for 12 h. After drying, the wt % of grafting GMA on to the fiber surface was calculated by measuring the weight of UHMWPE fiber before (w_1) and after (w_2) grafting process, according to eq. (1)[13]:

$$\%\ \mathrm{GMA}_r = [(w_2 - w_1)/w_1] \times 100 \quad (1)$$

Grafting of 5 wt % GMA on UHMWPE fiber was obtained as the values of w_1 and w_2 were measured to be 1.000 and 1.050 g, respectively.

Preparation of CNFs-Epoxy Nanocomposites

CNFs (0.5, 1, and 1.5% by weight of epoxy resin) were dispersed into the epoxy resin using ultrasonic energy in combination with a high-speed mechanical stirring. Ultrasonication was carried out in a cold water bath sonicator for 2.5 h. Mechanical stirring was carried out at 1500 rpm for 1 h at room temperature. Acetone was used to dilute the epoxy resin, due to its low boiling point and easy removal after processing. In this way, by reducing the chance of CNFs agglomeration, a good dispersion of CNFs in the epoxy resin was achieved. The vacuum was applied at 35 °C for 8 h to lessen the void and remove the solvent. The hardener was mixed manually with CNF/epoxy for 10 min in a cold water bath to avoid a further reaction. Then, the vacuum was again applied for 10 min to degasify the bubbles produced during the hardener mixing. Finally, the CNF/epoxy dispersions, containing 0.5, 1, and 1.5 wt % of GNFs were utilized in the UHMWPE single-fiber composite specimens.

Single Fiber Microdroplet Pullout Test

Samples Preparation. To evaluate interfacial adhesion between fiber and matrix, micromechanical tests (fragmentation, pullout, microdroplet, microindentation) are suggested.[28] In this study, microdroplet test was used to estimate average IFSS of fiber–matrix. Epoxy droplets containing different CNFs loading were deposited on the untreated and 5 wt % GMA-treated UHMWPE filaments by a needle syringe, according to the design of experiment in Table I.

Once deposited on to the UHMWPE fibers, the epoxy resin droplets were allowed to cure at room temperature for 24 h followed by a post treatment at 80 °C for 8 h. The droplets formed concentrically around the fiber in the shape of ellipsoids and retained their shape after appropriate curing. Once cured, the microdroplet dimensions and the fiber diameter were measured with the aid of an optical microscope (Motic-B3, UK). The embedded length was fixed by the diameter of the microdroplet along the fiber axis, which was dependent on the amount of resin deposited on the fiber. It is worthy to mention that the effect of various

Table I. Different Samples for Microdroplet Test

Sample code	GMA_r concentration (wt %)	CNF concentration (wt %)	CNF concentration (vol %)
A	0	0	0
B	5	0	0
C	0	0.5	0.39
D	5	0.5	0.39
E	5	1.0	0.78
F	5	1.5	1.17

concentrations of GMA on the IFSS of GMA-grafted UHMWPE fibers and epoxy resin was investigated in previous our work, which showed that the higher amount of GMA was grafted on UHMWPE fiber surface, the lower fiber properties would be. As a result of this, the lowest concentration as much as 5 wt % GMA was used here in order to avoid destruction of fiber nature by grafting procedure.[13]

Microdroplet Test. One end of each fiber specimen was glued to a paper tab, which could be easily connected to a load cell. The microdroplet specimens were then placed on the test machine (Zwick universal testing machine-1446 60, load cell 20 N), and the Vernier caliper's blades were used to grip the epoxy droplet. The gap between vernier caliper's blades was adjusted so that the fiber, but not the droplet, moved between them. The tensile loading rate was 1 mm/min. During the test, the force value and crosshead displacement were measured, and the load–displacement curve was recorded.

Micromechanical Analysis. The analysis of the results is based on micromechanics equations. Interfacial shear strength (IFSS) is calculated from the microdroplet test by eq. (2):

$$\tau_{app} = F_{max}/(\pi d_f L_e) \quad (2)$$

where d_f and L_e are the fiber diameter and embedded length of fiber, respectively. It is assumed that the shear stress is uniformly distributed along the embedded length.[29]

Gorbatkina[30] proposed the parameter of ultimate adhesive strength (τ_{ult}) more accurately to characterize the practical adhesion [eq. (3)]. This parameter is the shear stress required to produce ultimate shear failure (debonding) in a point at the interface.[30,31] This parameter accounts for the nonuniformity of the stress state along the interface, due to the end conditions and the loading.

$$\tau_{ult} = \{[\tau_{app} L_e \beta/\tanh(\beta L_e)) + (E_f d_f \beta/4)(\alpha_f - \alpha_m)\Delta T \ \tanh(\beta L_e/2]\} \quad (3)$$

where α_m and α_f are the coefficients of thermal expansion (CTE) of the matrix and fiber, respectively. ΔT is the variation of temperature ($\Delta T = T_{tes} - T_{stress\text{-}free}$), d_f is the fiber diameter, and E_f is the fiber Young's modulus. β is the shear-lag parameter that could be calculated by Cox's shear-lag analysis as follows:[32]

$$\beta = [8 \ G_m/E_f \ d_f{}^2 \ln(2r_m/d_f)]^{1/2} \quad (4)$$

where r_m is the droplet radius and G_m is the matrix shear modulus.

Some experimental studies[3,27] show that there is a slight increase in E_m (Young's modulus of the matrix) and G_m values of nano-epoxy materials over pure epoxy systems. Meanwhile, the CTE values of the all composites significantly decrease with CNF concentration. It is readily expected because the CTE of CNFs is much lower than that of the neat epoxy.[33] This decreasing trend leads to a smaller difference between CTE values of fiber and matrix, and consequently a downward trend for thermal stresses in the interface between UHMWPE fiber and matrix could be observed. Shokrieh *et al.*[33,34] calculated coefficient of thermal expansion (CTE) and Young's modulus of CNF-epoxy resin using micromechanical and modified micromechanical approaches according the following equations proposed by Schapery[34–36]:

$$\alpha_c = [\alpha_{nf} \ V_{nf} \ E_{nf} + \alpha_m(1 - V_{nf})E_m]/[V_{nf} \ E_{nf} + (1 - V_{nf})E_m] \quad (5)$$

$$E_c = [[1 + (2L_{nf}/d_{nf})\eta V_{nf}]E_m]/(1 - V_{nf}), \quad (6a)$$

$$\eta = [\gamma(E_{nf}/E_m) - 1]/[\gamma(E_{nf}/E_m) + (2L_{nf}/d_{nf})], \quad \gamma = 1/6 \ \text{(for nanofiber fillers)} \quad (6b)$$

where α, V, L, d, and E are thermal expansion coefficient, volume fraction, length, diameter, and elastic modulus, respectively. Also, the subscripts of c, nf, m indicate a composite (nanoepoxy system), nanofiller (CNF), and matrix (epoxy resin), respectively.

Measurements

The spectra of FTIR-ATR were obtained using an FTIR spectrometer (BOMEM MB-Series 100, Hartmann & Braun, Canada) with a Split Pea^{TM} accessory for ATR mode. Each obtained spectra was an average of 20 scans recorded at a resolution of 4 cm^{-1} in the range of 4000–650 cm^{-1}. The surface composition of the fibers was determined by X-ray photoelectron spectroscopy (XPS) on an ESCALAB 250 X-ray photoelectron spectrometer (Thermo Electron Corporation, USA) with monochromatized Al Ka X-ray source (1486.6 eV photons). Tensile properties of UHMWPE fibers were characterized using a Zwick universal testing machine (Model 1446-60, Germany) according to ASTM D3379-75.[29] The tension test was carried out at a constant loading rate (1 mm/min) until the filament fractures. 40 specimens were tested for each type of fiber. Apparent Young's modulus of the single UHMWPE fiber was also determined by this method, and all results were recorded. Surface properties of grafted UHMWPE fibers and the change of the microstructure due to the addition of CNFs were investigated using a scanning electron microscope (SEM; Philips-XI30, The Netherlands). The specimen mounts were coated with a thin layer of gold in an automatic sputter coater (KYKY-SBC 12, China) prior to examination by SEM.

Surface wettability was measured by static contact angle measurements on contact angle goniometry (Model OCA 15 PLUS, DATAPHYSICS) at room temperature. A 4 μL drop of distilled water was placed manually on to the molded resin surface and observed through a microscope. The experiments were

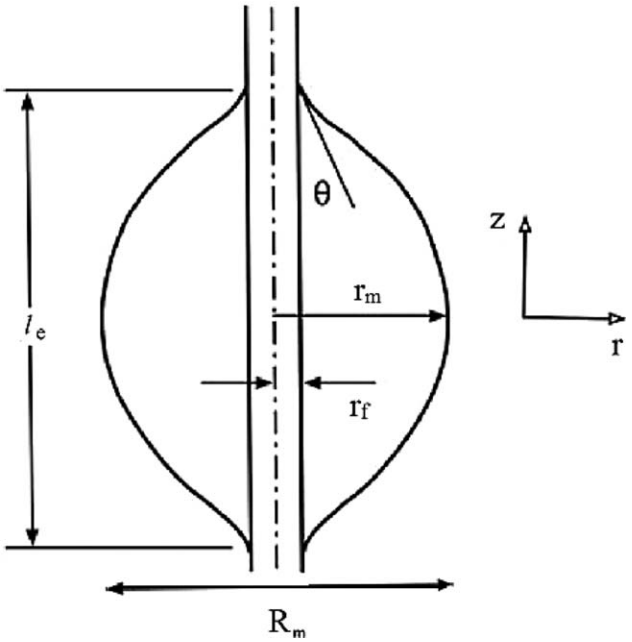

Figure 1. Schematic representation of a matrix drop deposited on a rigid fiber.[37]

conducted at 25 °C and 65% relative humidity. Fiber–matrix contact angles were also evaluated on the micro debonding specimens following an approach proposed by Carroll.[37] As schematically shown in Figure 1, the Laplace equations govern on the fiber shape [eq. 7(a,b)][37]:

$$-dr/dz=\sqrt{\left[(r_m^2-r^2)(r^2-a^2r_f^2)\right]}\Big/\left(r^2+ar_f r_m\right), \quad (7a)$$

$$a=\left(r_m\ \cos\theta-r_f\right)/\left(r_m-r_f\ \cos\theta\right) \quad (7b)$$

where r_f is the fiber radius, r_m is the maximum radius of the drop, θ is the contact angle, and r and z represent the radial and the longitudinal directions, respectively. By measuring r_f and r_m with an optical microscope, and integrating along the length L with an iterative procedure, the fiber–matrix contact angle (θ) could be evaluated according to eq. 7(a,b). A minimum of five microdroplets analyzed for each sample (Figure 1[37]).

RESULTS AND DISCUSSION

UHMWPE Fibers Characterizations

FTIR and XPS analysis were used to evaluate the surface chemical composition of the UHMWPE fibers. As shown in Figure 2(a), FTIR characteristic peaks of UHMWPE fibers appear at wavelengths of 2930–2850 cm^{-1} (—CH stretching) and 1460 cm^{-1} (—CH asymmetrical bending). Apart from XPS characteristics peak of C_{1s} in XPS spectra of pure UHMWPE fiber is presented in Figure 2(b), it shows an insignificant oxygen peak ascribed to the oxidation during the manufacturing process of fibers, which is not detected in its FTIR spectra. The presence of the polymerized GMA chains on the UHMWPE fibers surface could be deduced from appearance of FTIR peaks of carbonyl groups and epoxide rings at 1740 and 910 cm^{-1}, respectively. It is also confirmed by an intense peak of O_{1s} observed in its wide-scan XPS spectra [see Figure 2(b), (ii)]. After soaking the GMA-UHMWPE fiber into hardener solution, new peak of N_{1s} appears in its corresponding XPS spectra as well as FTIR absorption peaks of secondary N—H groups and secondary hydroxyl groups resulting from ring opening of epoxy groups in 1550 and 3700 cm^{-1} are observed, respectively, which clearly confirms successful reaction of GMA grafted on the fiber surface with hardener, which could bridge fiber surface with epoxy matrix.

SEM micrographs of UHMWPE fibers surface are shown in Figure 2(c). It could be observed that grafting of fiber surface causes a remarkable change in the surface topography of UHMWPE fibers. Apparently, the surface of the as-received fiber is smooth with some micro pits [Figure 2(c), (i)], while the surface of the GMA-grafted fibers is rough and some protuberances could be seen on its surface [Figure 2(c), (ii)].

As mentioned before, polyethylene is nonpolar and hydrophobic. Therefore, its surface energy is quite small and it requires improving its wettability with epoxy resin. Using polymerization of GMA on to the fiber surface, covalent bonds between fiber and matrix could be formed, and the interfacial adhesion is improved significantly.[12,13,38] Contact angles between UHMWPE fibers and epoxy resin, as well as aspect ratios (ratio of resin droplet diameter to embedded length (R_m/l_e), see Figure 1), are summarized in Figure 2(d). The results indicates that the fiber/matrix contact angle value, which was obtained by Carroll's equation, decreases from 77.1° to 51.5° after chemical grafting of GMA, which means that the wettability of the grafted fibers increases. Moreover, the aspect ratio (R_m/l_e) shows a significant reproducibility between samples correlating with the trend followed by fiber/matrix contact angles. In other words, the aspect ratio of UHMWPE/epoxy microcomposite (~1.07) is higher than that of GMA-UHMWPE/epoxy (~0.75). To conclude, chemical grafting of GMA leads to increases in higher fiber surface roughness and polarity resulting in better fiber/matrix wettability.

Tensile tests were conducted to determine the strength of a single fiber (before and after surface modification) and ensure that the UHMWPE fibers were unscathed after GMA grafting. As shown in Table II, there is a reduction in tensile properties of GMA-grafted UHMWPE fibers compared to unmodified fibers. According to literature, it is highly likely that the properties of the UHMWPE fibers would be slightly affected during surface chemical treatments. It is argued that the treatment of UHMWPE fibers surface via free radical GMA grafting could cause unwanted physical and mechanical changes because of thermal history excreted in the grafting process.[15,39,40] For example, Cartier *et al.*[41] showed that heating required for GMA treatment of UHMWPE fiber would induce melting and recrystallization as same as heating treatment of pure UHMWPE fibers. Nonetheless, they observed that the free radical grafting of GMA led to a slight decrease in the crystallinity of the fibers. They hypothesized that this phenomenon might be as a result of polyethylene chain branching.

CNFs-Epoxy Characterizations

The dispersion behavior of CNFs changes considerably with its concentration as well as the viscosity of the epoxy resin. Hence, selection of a suitable dispersion route for a particular

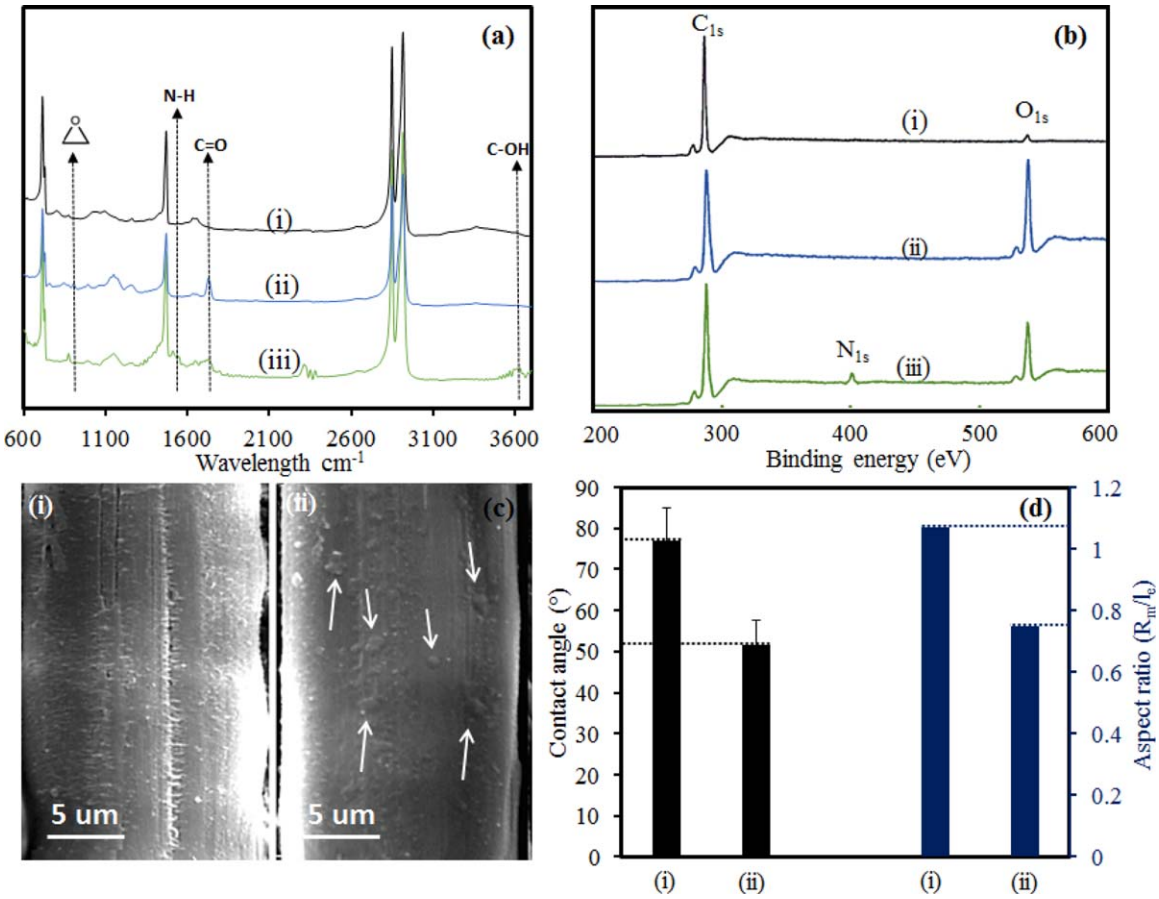

Figure 2. The FTIR-ATR spectra (a), XPS spectra (b), surface SEM images (c), and contact angle results (d) of as-received UHMWPE fiber (i), GMA-grafted UHMWPE fiber (ii), and GMA-grafted UHMWPE fiber after reaction with hardener (iii). [Color figure can be viewed in the online issue, which is available at wileyonlinelibrary.com.]

CNF-epoxy system is very much crucial since improper distribution leads to deterioration of composite properties. Some recent investigations show that the combination of ultrasonication and mechanical stirring are the most efficient technique to disperse 0.5 wt % CNFs or higher percentages and improve tensile properties of epoxy systems.[3,5] The treatment duration of both ultrasonication and mechanical stirring should be optimized to ensure minimum CNF breakage. In our study, 2.5 h of ultrasonic treatment was used in combination with 1 h of mechanical stirring to disperse 0.5, 1.0, and 1.5 wt % CNFs into the epoxy resin. The optical microscope was used to investigate the dispersion state of CNFs in the matrix (Figure 3). It could be noticed that the above-mentioned method leads to a very uniform dispersion of 0.5 wt % CNFs [Figure 3(a)]. Only a few small CNF agglomerates or clusters are presented in the dispersion of 1 wt % CNFs [Figure 3(b)]. While large agglomerates are visible in the dispersion of 1.5 wt % CNFs [Figure 3(c)], as indicated by the arrow. These agglomerations formed at higher contents of CNFs lead to a decrease in composite properties. Furthermore longer sonication treatment could damage CNFs resulting in curtailment of CNFs.[22,42]

The wetting behavior of CNF-epoxy resin surface by the water droplets was characterized by the water droplet contact angle test [Figures 3(d,d)]. Improved adhesion between the nonpolar UHMWPE fiber and the polar epoxy resin was pursued by altering either the surface of the fiber or the composition of the matrix. By developing a hydrophobic matrix material (through the addition of CNFs), the surface tension of epoxy resin decreases and fiber–matrix bonding could be improved.[38] It could be observed that the addition of CNFs causes an increment of the contact angle between water and resin. It implies a more hydrophobicity for CNF–epoxy nanocomposites compared

Table II. Tensile Properties of a Single UHMWPE Fiber before and after GMA Grafting

Fiber type	Fiber diameter (μm)	Tensile strength (MPa)	E-modulus (GPa)	Strain at break (%)
As-received	21.0	2700 ± 135	89.0 ± 3.8	3.5 ± 0.20
GMA treated	18.7	2210 ± 145	87.9 ± 2.3	3.0 ± 0.26

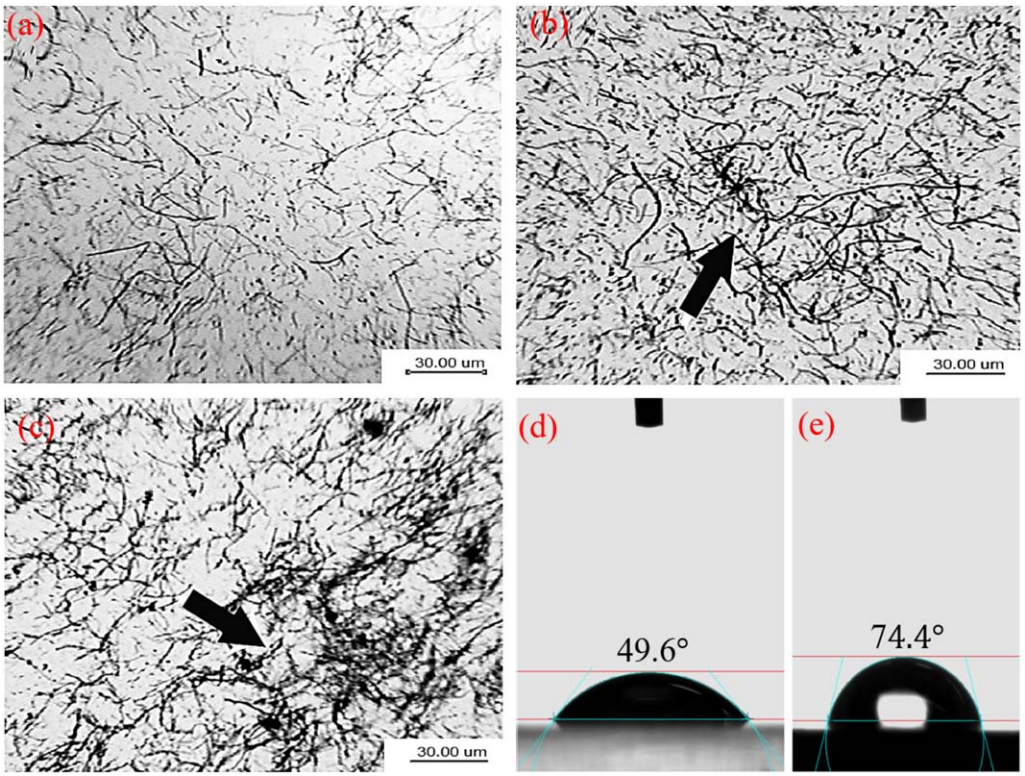

Figure 3. Dispersion of 0.5 wt % (a), 1 wt % (b), and 1.5 wt % CNF (c) into epoxy resin as observed by an optical microscope; and the static contact angles of water droplets on pure epoxy (d), and 0.5 wt % CNF-epoxy nanocomposite (e). [Color figure can be viewed in the online issue, which is available at wileyonlinelibrary.com.]

to the neat epoxy. In fact, the CNFs make the epoxy nonpolar, as the same as nonpolar UHMWPE fiber. Therefore, it is hypothesized that this procedure makes these two substances more compatible especially when the fiber is treated with low amount of GMA, which results in better wetting and adhesion of fiber and matrix.

Interfacial Shear Strength Analysis

Figure 4 presents the force–displacement curves obtained in our microdroplet tests. Linear behavior corresponding to elastic energy storage is observed until the force reaches the maximum value (F_{max}). Once F value reaches to F_{max}, debonding appears and the energy previously stored is released through fast interfacial cracking with a nearly constant friction force. From this moment, only friction interactions occur.[43] A 'kink' phenomenon has been identified in the force–displacement results of microdroplet tests by other researchers.[44] According to Figure 4, no clear 'kink' point in the force–displacement curves is observed for the samples A and C, suggesting that the debonding occurs suddenly at smaller forces, and there is no stable crack. In contrast, both GMA-treated UHMWPE fiber and CNF-epoxy systems (samples B and D) caused definite 'kink' points in the force–displacement curves. This indicates a mixed adhesive and cohesive character of interfacial failure resulting in a better stress-transfer ability up to high loads before a first crack starts to grow. In other words, the matrix modfication or fiber treatment could cause the series of small intense failures preventing from becoming catastrophic debonding.

Additionally, the forces required for the crack initiation and ultimate debonding in the samples B and D are higher that those of samples A and C. It could be argued that the action of CNFs as bridges, alongside fiber treatment, to change the crack propagation path could result in higher friction energy.[3]

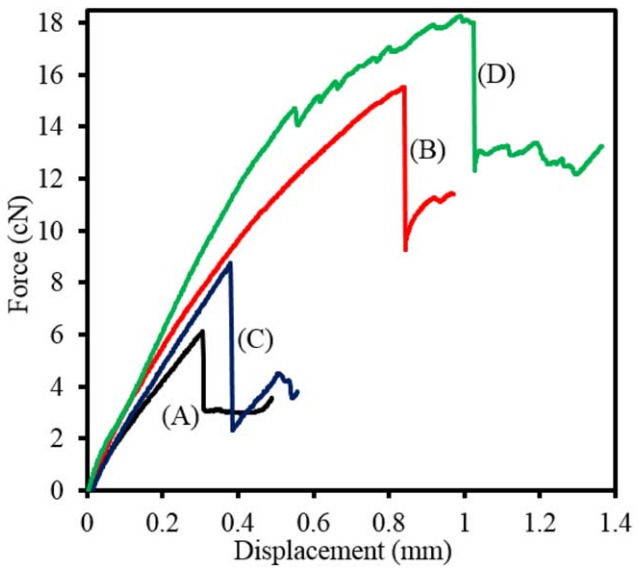

Figure 4. The force–displacement curves from microdroplet tests (the sample codes are according to Table I). [Color figure can be viewed in the online issue, which is available at wileyonlinelibrary.com.]

Table III. Coefficient of Thermal Expansion (CTE) and Tensile Modulus of Composite Components

Components	CTE (10^{-6}/°C)	E-modulus (GPa)
Epoxy resin	70	2.52
UHMWPE fiber	−13.12	89.0 (3.8)[a]
5% GMA-grafted fiber	−13.10	87.9 (4.5)
Carbon nano fiber (CNF)	−1	240

[a] Standard deviation (SD).

Table IV. Coefficient of Thermal Expansion (CTE) and Tensile Modulus of CNF-Epoxy Composite

CNF conc. (wt %)	CTE (10^{-6}/°C)	E-modulus (GPa)
0 (pure epoxy resin)	70.0	2.52 (0.12)[a]
0.5	53.6	2.57 (0.14)
1.0	43.3	2.62 (0.10)
1.5	36.3	2.78 (0.13)

[a] Standard deviation (SD).

It is necessary to characterize the adhesion between fiber and matrix quantitatively to control the interfacial strength. Therefore, the data recorded during debonding tests were analyzed using the micromechanics equations. The apparent interfacial strength (τ_{app}) and the ultimate strength (τ_{ult}) were calculated from eqs. (2) and (3), respectively. According to eq. (3), τ_{ult} depends on external stress or load applied to UHMWPE fiber and thermal stress due to different coefficients of thermal expansion (CTE) of the fiber and matrix. The values of Young's modulus and CTEs of the composite components are reported in Table III.

Compared with the epoxy matrix, CNFs have much higher Young's modulus and much lower CTE. Therefore, dispersion of this nano-additive into epoxy matrix makes its properties closer to the fiber ones, and consequently reduces the residual stresses in fiber-reinforced composites.[19,45] It could be also seen that the UHMWPE fiber has a negative linear thermal expansion coefficient in the fiber direction. The linear thermal expansion coefficient of GMA-treated fibers could be estimated from the relation between the thermal expansion coefficients and tensile modulus of UHMWPE fiber.[46,47] The CTE of the neat epoxy resin and CNF/epoxy specimens (at three different weight fractions of CNFs) were calculated to investigate the CNFs effects on CTE of epoxy using eqs. 5 and 6. The CTE values and the averaged tensile test results are shown in Table IV.

The results show that adding CNFs to the epoxy resin has a slight impact on the matrix Young's modulus. In other words, the inclusion of 1.5 wt % of CNFs in epoxy matrix could increase Young's modulus only ~10%, compared with neat epoxy. On the contrary, it is observed that the CTE values of all the composites significantly decrease with increase of CNFs loading, which is because of the much lower CTE value of CNFs in comparison with neat epoxy. In fact, the significant reduction of CTE of polymer reinforced with nanoadditives could be attributed to a large interfacial area between the nanoadditives and the matrix, a strong interface bonding, and a good impregnation of the nanoadditives with the matrix.[33]

The calculated results for apparent interfacial shear strength and ultimate adhesive strength for 5 wt % GMA-treated UHMWPE/CNF-epoxy composites with different concentrations of CNFs (0.5–1.5 wt %) are shown in Table V. It is observed that 5 wt % GMA grafting of fiber surface (sample B) increases the apparent interfacial shear strength (τ_{app}) by 197% in comparison with as-received fiber reinforced epoxy resin (sample A). This observation could be explained by chemical bonds formed at the UHMWPE fiber–epoxy resin interface, between epoxy groups of GMA and epoxy groups in the matrix attached to each other via diamine hardener. On the other hand, compared with fiber treatment (sample B), it could be deduced that matrix modification (sample C) is less effective. In other words, ~9% increase is observed for sample C, compared with sample code A. It is due to the fact that matrix modification could improve interfacial adhesion through mechanical interlocking, which could physically restrict fiber movement during pulling out process. However, fiber treatment helps interfacial adhesion with chemical bonding.

It is shown that the interfacial adhesion of specimens with CNFs-epoxy matrices (samples D, E, and F) have increased about 319, 306, and 291% respectively, in comparison with samples with the pure epoxy matrix. The CNFs are likely to interlock and entangle with the polymer chains in the matrix. Thus, the addition of CNFs enhances the crosslinking between polymer chains and provides better interfacial bonding. The presence of CNFs increases the crack propagation resistance and prevents crack generation by bridging effect at the interface region of UHMWPE fiber, CNF, and epoxy matrix. Moreover, CNFs have a high aspect ratio, which improves the strength and modulus of epoxy polymer.[48,49] Nonetheless, compared with sample D containing 0.5 wt % of CNFs, a higher concentration of CNFs does not lead to better interfacial properties (samples E and F contains 1 and 1.5 wt % of CNFs). It might be due to the creation of microaggregates of CNFs in various regions of the polymer matrix, which act as areas of weakness.[3,48]

A clear synergy between UHMWPE fibers treatment and CNFs-epoxy matrix is observed resulting in improvements beyond the

Table V. Interfacial Shear Strength (Apparent and Ultimate) of GMA-Grafted UHMWPE Fiber Reinforced CNF–Epoxy Nanocomposites (see Table I for Sample Codes)

Sample code	l_e/R_m	τ_{app} (MPa)	τ_{ult} (MPa)
A	0.93 (0.1)[a]	1.93 (0.95)	23.10 (6.40)
B	1.33 (0.04)	5.74 (1.85)	45.44 (14.20)
C	1.14 (0.10)	2.10 (0.89)	23.74 (5.46)
D	1.49 (0.08)	8.10 (1.97)	53.62 (13.42)
E	1.46 (0.06)	7.85 (1.58)	53.14 (14.36)
F	1.45 (0.05)	7.55 (1.81)	53.03 (12.94)

[a] Standard deviation (SD).

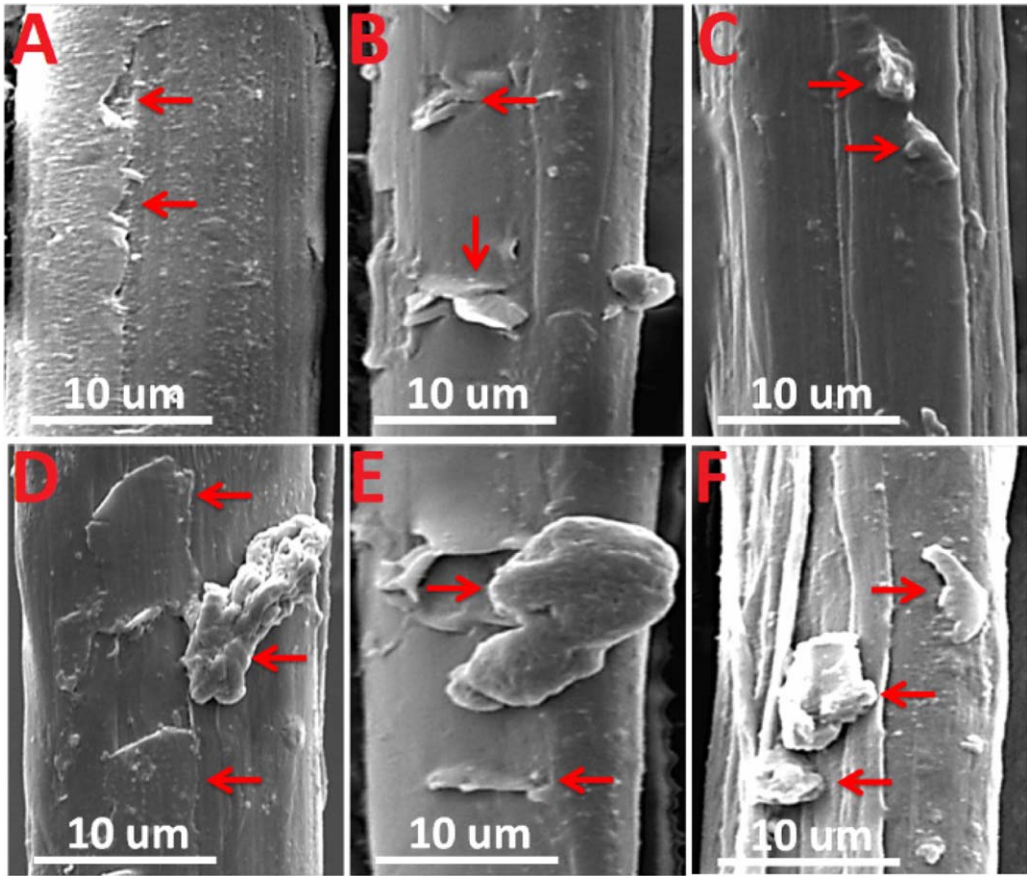

Figure 5. SEM images of the failure surface from different samples after a microdroplet test (see Table I for sample codes). [Color figure can be viewed in the online issue, which is available at wileyonlinelibrary.com.]

additive effect causing by either matrix modification or fiber surface treatment. The τ_{app} has been improved significantly from 1.93 MPa for epoxy model composite containing as-received UHMWPE fibers (sample A) to 8.1 MPa for 0.5 wt % CNF-epoxy nanocomposites consisting of 5 wt % GMA-grafted UHMWPE fibers (sample D). The interfacial reinforcing mechanisms of these nanocomposites (both fiber treatment and matrix modification) could be interpreted as covalent bonding, van der Waals binding, mechanical interlocking, and surface wetting.[50] Although the results show that the ultimate strength values are significantly higher than the apparent shear strength, the same trend as the apparent shear strength is observed for ultimate strength values of different samples. Ultimate adhesive strength above-calculated is considered as the intrinsic interface property characterizing the interfacial strength of UHMWPE and matrix from an engineering viewpoint. This property could also be associated with the action of molecular forces, and nature and surface density of adhesion bonds at molecular levels. Analysis of this relationship allows us to differentiate the components of the local bond strength, as well as to estimate distances characteristic of interactions. Compared with apparent interfacial shear strength, thermal stress residues play an important role in ultimate adhesive strength. In other words, as shown in Table V, compared with nontreated composites (sample code A), an increase ~96.7% in (τ_{ult}) is observed for the sample containing GMA-treated fiber (sample code B). However, for apparent interfacial shear strength, this could be estimated ~197%. It means that thermal stresses play an undeniable role in interfacial adhesion. The same observation could be seen for the other samples. Additionally, it is hypothesized that addition of CNFs could reduce residual thermal stresses. To put it differently, compared with GMA-treated fiber reinforced composites containing pure epoxy as a matrix (sample B), GMA-treated UHMWPE fibers/CNFs-epoxy specimens (samples D, E, and F) show higher ultimate adhesive strengths and lower residual thermal stresses. The earlier investigation reported by Chandra *et al.*[51] has extensively discussed the reasons for modification of thermal properties of polymer by inclusion of nanomaterial, such as CNFs.

SEM Analysis

SEM was used to observe the failure surfaces of the specimens after the microdroplet test (Figure 5). For conventional composite shown in Figure 5(A), the surface of the fiber is clean, and no matrix adheres to the fiber. The fracture surface of fiber is flat, and some cracks are observed on the fiber side near the fiber–matrix interface. In other words, interfacial failure occurs indicating that the interfacial bonding between the fiber and matrix is weak. The adhesion of fiber to the matrix shows improvement in the GMA-grafted fiber composite [Figure 5(B)] due to chemical bonds formed between epoxy groups of GMA and epoxy groups in the matrix. The presence of epoxy adhered

to the fiber surface also suggests that interfacial adhesion is stronger than matrix strength in composites.[52] The fracture surface of the nanocomposite [Figure 5(C)] shows that the matrix surface is rougher than that of the neat composite. Additionally, as shown in Figure 5(D–F), the epoxy resin appears to cling to fibers well.

The failure in the GMA-treated UHMWPE fibers/CNFs-epoxy specimens runs along the interphase and combines both cohesive failure in epoxy resin (the presence of some fragments) and adhesive failure as some bare fiber surfaces could be seen. However, cohesive failure is dominated in samples D, E, and F. The interfacial area between the matrix and CNFs increases because of the high aspect ratio of the CNFs, which in turn leads to better mechanical properties.[53] In fact, both CNFs and fibers are stronger than a matrix. Therefore, when load is applied to the composite structures, matrix starts to crack firstly and stress is then transferred from the lower modulus matrix to the CNFs and then to the long fiber, ultimately resulting in enhancement of the properties of composite systems.[48]

CONCLUSIONS

The effect of simultaneous fiber surface modification and matrix modification on the interfacial properties of UHMWPE fiber/epoxy model microcomposites was characterized. The fiber surface was treated by grafting of polyGMA chains while epoxy matrix was modified by incorporation of CNFs. The highest interfacial shear strengths (apparent and ultimate), better dispersion, and improved wettability were obsereved for the samples containg 0.5 wt % CNFs. Such observations proved that the combination of GMA-grafted UHMWPE fibers and modified epoxy could have synergestic effect on adhesion with improvements of up to 319% in the apparent interfacial shear strength, compared with pure sample. Such improvement was arising from the formation of various interactions at the fiber/matrix interface namely chemical interactions between the functional groups of GMA and epoxy, as well as mechanical interlocking. CNFs infusion even at quite low concentrations enhanced the mechanical properties of the composite system. As matrix was reinforced with CNFs, the CNFs could conjoin matrix with UHMWPE fibers through mechanical interlocking resulting in better interfacial bonding. The SEM micrographs of the debond sites showed that the simultaneous surface treatment of fiber and matrix modification resulted in a failure mode transition from adhesive to cohesive failure.

REFERENCES

1. Zhang, Q.; Wang, Q.; Chen, Y. J. *Appl. Polym. Sci.* **2013**, *130*, 3930.
2. Song, K.; Zhang, Y.; Meng, J.; Green, E. C.; Tajaddod, N.; Li, H.; Minus, M. L. *Materials* **2013**, *6*, 2543.
3. Zhong, W. H.; Sui, G.; Jana, S.; Miller, J. *Compos. Sci. Technol.* **2009**, *69*, 2093.
4. Cartwright, B. K.; Mulcahy, N. L.; Chhor, A. O.; Thomas, S. G.; Suryanarayana, M.; Sandlin, J. D.; Crouch, I. G.; Naebe, M. *J. Manuf. Sci. Eng.* **2015**, *137*, 051011.
5. Zheng, Z.; Huang, X.; Li, Y.; Yang, N.; Wang, X.; Shi, M. *Compos. B: Eng.* **2012**, *43*, 1538.
6. Lin, S. P.; Han, J. L.; Yeh, J. T.; Chang, F. C.; Hsieh, K. H. *J. Appl. Polym. Sci.* **2007**, *104*, 655.
7. Yakusheva, D.; Yakushev, R.; Oschepkova, T.; Strelnikov, V. *J. Appl. Polym. Sci.* **2011**, *122*, 1628.
8. Koronis, G.; Silva, A.; Fontul, M. *Compos. B: Eng.* **2013**, *44*, 120.
9. Laghaei, M.; Sadeghi, M.; Ghalei, B.; Dinari, M. *Prog. Org. Coat.* **2016**, *90*, 163.
10. Warrier, A.; Godara, A.; Rochez, O.; Mezzo, L.; Luizi, F.; Gorbatikh, L.; Lomov, S. V.; VanVuure, A. W.; Verpoest, I. *Compos. A: Appl. Sci.* **2010**, *41*, 532.
11. Zabihi, O.; Ahmadi, M.; Akhlaghi bagherjeri, M.; Naebe, M. *RSC. Adv.* **2015**, *5*, 98692.
12. Ahmadi, M.; Masoomi, M.; Safi, S. *Compos. B: Eng.* **2015**, *83*, 43.
13. Sadeghi Broujerdi, M.; Masoomi, M.; Asgari, M. *J. Reinf. Plast. Compos.* **2013**, *32*, 1675.
14. Li, Z.; Zhang, W.; Wang, X.; Mai, Y.; Zhang, Y. *Appl. Surf. Sci.* **2011**, *257*, 7600.
15. Wang, J.; Liang, G.; Zhao, W.; Lü, S.; Zhang, Z. *Appl. Surf. Sci.* **2006**, *253*, 668.
16. Zhao, J.; Guo, Z.; Liang, G.; Wang, J.; Zhang, G. *J. Appl. Polym. Sci.* **2005**, *9*, 1011.
17. Yakusheva, D. E.; Oshchepkova, T. E.; Yakushev, R. M.; Strel'nikov, V. N. *Russian J. Appl. Chem.* **2010**, *83*, 1403.
18. Rodriguez, A. J.; Guzman, M. E.; Lim, C. S.; Minaie, B. *Carbon* **2011**, *49*, 937.
19. Sun, L. H.; Ounaies, Z.; Gao, X. L.; Whalen, C. A.; Yang, Z. G. *J. Nanomater.* **2011**, 1.
20. Green, K. J.; Dean, D. R.; Vaidya, U. K.; Nyairo, E. *Compos. A: Appl. Sci.* **2009**, *40*, 1470.
21. Zhang, G.; Karger-Kocsis, J.; Zou, J. *Carbon* **2010**, *48*, 4289.
22. Rana, S.; Alagirusamy, R.; Fangueiro, R.; Joshi, M. *J. Appl. Polym. Sci.* **2012**, *125*, 1951.
23. Zabihi, O.; Aghaie, M.; Zare, K. *Therm. Anal. Calorim.* **2012**, *111*, 703.
24. Zabihi, O.; Khodabandeh, A.; Ghasemlou, S. *Polym. Degrad. Stabil.* **2012**, *97*, 1730.
25. Salehi-Khojin, A.; Stone, J. J.; Zhong, W. H. *J. Compos. Mater.* **2007**, *41*, 1163.
26. Zhu, J.; Wei, S.; Ryu, J.; Budhathoki, M.; Liang, G.; Guo, Z. *J. Mater. Chem.* **2010**, *20*, 4937.
27. Xu, L. R.; Bhamidipati, V.; Zhong, W. H.; Li, J.; Lukehart, C. M. *J. Compos. Mater.* **2004**, *38*, 1563.
28. Moon, C.; Holmes, G.; McDonough, W. *J. Appl. Polym. Sci* **2007**, *105*, 3483.
29. Kang, S. K.; Lee, D. B.; Choi, N. S. *Compos. Sci. Technol.* **2009**, *69*, 245.
30. Gorbatkina, A. Adhesion Strength of Fiber–Polymer Systems; Ellis Horwood: New York, **1992**.

31. Pisanova, E.; Zhandarov, S.; Mader, E.; Ahmad, I.; Young, R. *J. Compos. A: Appl. Sci.* **2001**, *32*, 435.
32. Zhandarov, S.; Pisanova, E.; Lauke, B. *Compos. Interface* **1998**, *5*, 387.
33. Shokrieh, M. M.; Daneshvar, A.; Akbari, S.; Chitsazzadeh, M. *Carbon* **2013**, *59*, 255.
34. Schapery, R. A. *J. Compos. Mater.* **1968**, *2*, 380.
35. Hsiao, K. T. *Compos. A: Appl. Sci.* **2008**, *39*, 834.
36. Gonnet, P. Thermal Conductivity and Coefficients of Thermal Expansion of SWNTS/Epoxy Nanocomposites; Florida State University, **2004**.
37. Miller, B.; Gaur, U.; Hirt, E. *D. Compos. Sci. & Tech* **1991**, *42*, 207.
38. Jackson, D. C. Engineering Polyethylene Surface Energy for Adhesion; University of Florida: Florida, **2011**.
39. Sa, R.; Wei, Z.; Yan, Y.; Wang, L.; Wang, W.; Zhang, L.; Ning, N.; Tian, M. *Compos. Sci. Technol.* **2015**, *113*, 54.
40. Xing, Z.; Wang, M.; liu, W.; Hu, J.; Wu, G. *Radiat. Phys. Chem.* **2013**, *86*, 84.
41. Cartier, H.; Hu, G. H. *J. Polym. Sci. A: Polym. Chem.* **1998**, *36*, 2763.
42. Bhattacharyya, A.; Rana, S.; Parveen, S.; Fangueiro, R.; Alagirusamy, R.; Joshi, M. *J. Appl. Polym. Sci.* **2013**, *129*, 2383.
43. Zhandarov, S.; Mäder, E. *Compos. Sci. Technol.* **2005**, *65*, 149.
44. Mäder, E.; Gao, S.; Plonka, R. *Compos. Sci. Technol.* **2007**, *67*, 6.
45. Chandra, A.; Meyer, W. H.; Best, A.; Hanewald, A.; G.,W. *Macromol. Mater. Eng.* **2007**, *292*, 295.
46. Yamanaka, A.; Kashima, T.; Tsutsumi, M.; Ema, K.; Izumi, Y.; Nishijima, S. *J. Compos. Mater.* **2007**, *41*, 165.
47. Kashima, T.; Yamanaka, A.; Takasugi, T.; Nishihara, Y. *Adv. Cryogenet. Eng.* **2000**, *46*, 329.
48. Hossain, M. K.; Hossain, M. E.; Hosur, M. V.; Jeelani, S. *Compos. A: Appl. Sci.* **2011**, *42*, 1774.
49. Naebe, M.; Abolhasani, M. M.; Khayyam, H.; Amini, A.; Fox, B. *Polym. Rev.* **2016**, *56*, 31.
50. Zhang, F. H.; Wang, R. G.; He, X. D.; Wang, C.; Ren, L. N. *J. Mater. Sci.* **2009**, *44*, 3574.
51. Lubineau, G.; Rahaman, A. *Carbon* **2012**, *50*, 2377.
52. Gao, X. Tailored Interphase Structure for Improved Strength and Energy Absorption of Composites; The University of Delaware: Delaware, **2006**.
53. Tsantzalis, S.; Karapappas, P.; Vavouliotis, A.; Tsotra, P.; Paipetis, A.; Kostopoulos, V.; Friedrich, K. *Compos. A: Appl. Sci.* **2007**, *38*, 1076.